Korean J. Chem. Eng., 33(7), 2215-2221 (2016)
DOI: 10.1007/s11814-016-0067-9

pISSN: 0256-1115
eISSN: 1975-7220

Effect of pyrolytic temperature on the adsorptive removal of p-benzoquinone, tetracycline, and polyvinyl alcohol by the biochars from sugarcane bagasse

Guoting Li†, Weiyong Zhu, Lingfeng Zhu, and Xiaoqi Chai

Department of Environmental and Municipal Engineering, North China University of Water Resources and Electric Power, Zhengzhou 450011, China

(*Received 15 October 2015 • accepted 4 March 2016*)

Abstract−Sugarcane bagasse was pyrolyzed under oxygen-limited conditions from 100 to 600 °C and used for the adsorptive removal of oxidation intermediate p-benzoquinone, tetracycline, and polyvinyl alcohol. The three organic pollutants have different polarities and solubilities. The carbon content increased from 57.7% of the raw bagasse to 75.3% of the biochar pyrolyzed at 600 °C, while the O content decreased from 13.2% to 6.1%. Accordingly, the biochar surface became more hydrophobic with increasing pyrolytic temperature. Interestingly, the adsorption affinity of biochars towards the three pollutants improved with an increase in the pyrolytic temperature. The adsorption of tetracycline molecules was almost unaffected by its being negatively charged with increasing solution pH. A mechanism of π-π electron-donor-acceptor interaction might contribute to the adsorption of tetracycline and p-benzoquinone, while H-bond interaction between polyvinyl alcohol and the biochar might be dominant during adsorption. The Elovich model fitted the kinetic model well, indicating that the diffusional rate-determining step was more pronounced. An isotherm study indicated that the contribution of partitioning was also dominant in the adsorption processes. Wide application of the prepared biochars is expected for the efficient adsorptive removal of organic pollutants.

Keywords: Biochar, Sugarcane Bagasse, Pyrolytic Temperature, Adsorption, Micropollutants

INTRODUCTION

Emerging micropollutants such as pharmaceutical and personal care products (PPCPs) have aroused worldwide attention in recent years due to their acute long-term effects on the environment and the human body [1,2]. Addressing these problems will necessitate a number of new methods of purifying water at lower cost and with less energy, while at the same time minimizing the use of chemicals and the impact on the environment [3]. Owing to the ineffectiveness of conventional physico-chemical and biological techniques for micropollutant removal, such as sand filtration, sedimentation, flocculation, and coagulation [4], an increasing number of advanced oxidation processes (AOPs) have emerged as alternative technologies for the effective removal of these organic micropollutants [5]. AOPs are all characterized by the production of powerful, and highly reactive, oxygen species such as OH radicals (2.8 V/NHE), which degrade aromatic pollutants to a series of oxidation intermediates including p-benzoquinone, catechol, and hydroquinone. Nonetheless, it is neither practical nor economical to transform all the reaction intermediates into water, and carbon dioxide as a very long reaction is usually required for AOPs [6]. Meanwhile, one major concern with AOPs is that the toxicity of degradation intermediates, such as catechol and quinones, might become higher than their parent chemicals [7]. For example, it was reported that hydroquinone and p-benzoquinone were, respectively, three, and two, orders of magnitude more toxic than their parent phenol. From a practical point of view, AOPs alone could not completely reduce, or even eliminate, the toxicity of aromatic pollutants and their oxidation intermediates. There is a pressing need to find other techniques to help AOPs or remove these chemicals involved independently.

Typically, adsorption processes could transfer these pollutants from one phase to another efficiently, with no toxic intermediates generated [8-12]. The integration of AOPs with the subsequent adsorption process might be a good option for the complete removal of these micropollutants. Concurrently, some carbonaceous sorbents have demonstrated strong capabilities towards the adsorptive removal of micropollutants such as tetracycline [13] and polyvinyl alcohol (PVA) [14].

Biochars have demonstrated practical applications in solving a series of environmental problems. On the one hand, biochar offers the chance to turn bioenergy into a carbon-negative industry. As it can be assumed that about 3.5 t ha^{-1} y^{-1} of biomass are in the USA alone, low-temperature pyrolysis, with carbon sequestration and gas capture, are expected to be a carbon-neutral energy source [15, 16]. On the other hand, biochar is being used in environmental management including soil improvement, waste management, climate change mitigation, and energy production [17]. In particular, biochar has potential for application as an eco-friendly sorbent for soil and water contaminated with organic/inorganic substances. Low-temperature pyrolysis is usually used to convert biomass, typically agricultural waste, into biochars [18]. Not only can the increased pyrolytic temperature increase the carbon content, but also improve the thermal stability of the biochars [19]. It is reported that

†To whom correspondence should be addressed.
E-mail: liguoting@ncwu.edu.cn, lipsonny@126.com

the structural, and surface, characteristics of biochars of orange peel were significantly regulated by pyrolytic temperature [20]. As adsorption mechanisms, such as transitional adsorption and partition, would occur on the biochars produced at different temperatures [21,22], the uptake of pollutants is expected to be significantly influenced by the pyrolytic temperature.

We used sugarcane bagasse as the raw material to produce a biochar under different temperatures. The performance of the resultant biochar was investigated with regard to its adsorptive removal of p-benzoquinone, tetracycline, and PVA. The adsorption kinetics and isotherms for the three pollutants, with different polarities and solubilities, were compared. As stated above, p-benzoquinone is one of the indispensable oxidation intermediates generated in AOPs. Additionally, tetracycline is typical of the PPCPs occurring in natural waters, while PVA is a recalcitrant polymer pollutant present in the environment. They have different water solubilities and polarities. It can be expected that their adsorption performance by biochars might differ significantly.

MATERIALS AND METHODS

1. Materials

The p-benzoquinone (chemical purity) was purchased from Beijing Chemical Reagent Company, and used without further purification. Polyvinyl alcohol (PVA, 95.5%) was provided by Kemio Chemical Reagent Company (Tianjin, China), and tetracycline was purchased from Hefei Bomei Biological Science and Technology Co., Ltd. (Anhui Province, China). Both PVA and tetracycline were used without further purification. Other chemicals used were of analytical grade. Deionized (DI) water was used throughout the study.

2. Biochar Preparation

Sugarcane bagasse (bagasse) was collected from Guangxi Province, China. It was washed in water, dried under sunlight, and then ground and screened through a 100 mesh sieve. The obtained fine powder was then oven-dried at 80 °C and stored in a desiccator for further use. Biochars from bagasse were prepared by pyrolyzing biomass at various temperatures (100, 200, 300, 400, 500, and 600 °C) for 2 h. To maintain oxygen-limited conditions, the bagasse powder was placed in a ceramic pot in a compressed state, and covered with a tight-fitting lid.

For demineralization, the resultant biochars were placed in a 4 mol/L HCl solution for 12 h and separated by filtration. Then the residues were rinsed with DI water to neutral solution pH and oven-dried overnight at 80 °C. The treated biochars were finally passed through a 100 mesh sieve. These biochars were hereafter designated B100, B200, B300, B400, B500, and B600, respectively, wherein the suffix number represented the pyrolytic temperature.

3. Characterisation

The surface morphologies of raw bagasse and biochars pyrolyzed at different temperatures were characterized with a Philips Quanta-2000 scanning electron microscope (SEM) coupled with an energy dispersive X-ray (EDX) spectrometer. FTIR spectra (KBr pellets) were recorded on a Nicolet NEXUS 470 FTIR spectrophotometer from 400 to 4,000 cm^{-1}. A zeta potential analyser (Zetasizer 2000, Malvern, UK) was used to analyze the zeta potential of B600 over 3.0≤pH≤10.0.

4. Batch Adsorption Studies

In the batch adsorption study, adsorption tests were performed in a series of 100-mL conical glass flasks. In the flasks, 10 mg of sorbent was added to 50 mL solution with initial p-benzoquinone, tetracycline, and PVA concentrations of 5, 20, and 20 mg/L, respectively. These mixtures were shaken at 135 rpm for 24 h to achieve adsorption equilibrium based on the predetermined adsorption kinetics. The temperature was kept at 25 °C unless otherwise stated. For the pH effect study, solution pH adjustment was conducted by adding diluted HCl or NaOH solution. All solution pH values were maintained at neutral pH except during the pH effect study.

For the kinetic study, 200 mg of sorbent was added to 1,000 mL solution with initial p-benzoquinone, tetracycline, and PVA concentrations of 5, 20, and 20 mg/L, respectively. The mixed solution was stirred at a constant rate. The samples were collected at different time intervals. The adsorption isotherm studies were carried out with varying pollutant concentration.

5. Analysis Methods

Samples were collected and filtered through a 0.45 μm membrane before being analysed in a UVmini-1240 spectrophotometer (Shimadzu, Japan). The concentrations of p-benzoquinone and tetracycline were determined by measuring absorption at fixed wavelengths of 254 nm [23] and 360 nm [24], respectively. According to the procedures described by Finley [25], boric acid and iodine solutions were added to the pre-treated samples, and then the PVA concentration was determined by measuring the absorption at a fixed wavelength (690 nm) using the same spectrophotometer. The adsorption capacity was calculated using the following equation:

$$q_e=(C_0-C_e)\ V/W \quad (1)$$

where q_e (mg/g) is the adsorption capacity at equilibrium; C_0 and C_e (mg/L) are the initial and equilibrium concentrations of p-benzoquinone, tetracycline, and PVA in solution, respectively; V (L) is the volume of solution, and W (g) is the mass of adsorbent used.

RESULTS AND DISCUSSION

1. Characterization of Biochars from Sugarcane Bagasse

1-1. Surface Morphologies of Biochars Prepared from Bagasse

The morphologies (SEM) of raw bagasse, and bagasse pyrolyzed at 400 °C and 600 °C are shown in Fig. 1. As seen from Figs 1(a) and (b), the raw bagasse mainly consisted of thick, multi-layered flakes. After pyrolysis, thin flakes predominated and the thick flakes almost all disappeared. This demonstrated that pyrolysis cleaved the natural layers of the raw bagasse. Compared with the bagasse pyrolyzed at 400 °C, the flakes became smaller when the pyrolytic temperature increased to 600 °C (see Figs. 1(c) to (f)). The increased pyrolytic temperature generated smaller biochar flakes.

The C, N, and O content, and the molar ratios of O/C and (O+N)/C in the raw bagasse, and biochars pyrolyzed at 400 °C and 600 °C were roughly indicated by EDX as a reference (Fig. 2(a)). Evidently, raw bagasse, and biochars pyrolyzed at 400 °C and 600 °C were all carbon-rich, with carbon contents increasing from 57.7% of the raw bagasse to 75.3% of the biochar pyrolyzed at 600 °C. The carbon content of bagasse biochar in this research was especially

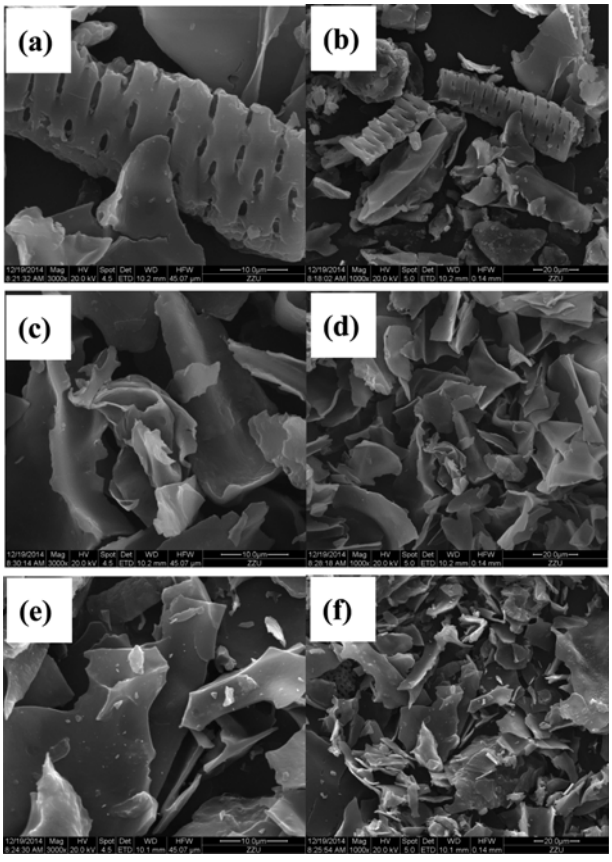

Fig. 1. SEM micrographs of raw bagasse (a), (b), and bagasse pyrolyzed under 400 °C (c), (d) and 600 °C (e), (f).

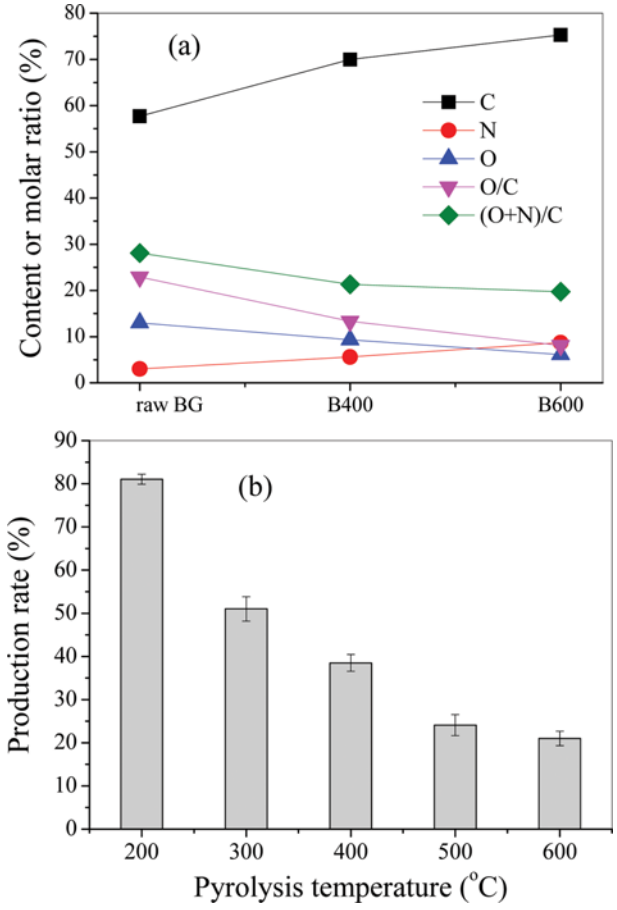

Fig. 2. Changes in element contents (wt%) of C, N, O and the molar ratios (%) of O/C and (O+N)/C in the raw bagasse, and biochars pyrolyzed under 400 °C and 600 °C (a) and production rates of biochar samples prepared under different pyrolysis temperatures (b).

close to that of bagasse biochar (76.5%) treated by pyrolysis in an N_2 environment at 600 °C as evidenced by elemental analysis [26]. Besides, the N content increased gradually from 3.0% of the raw bagasse to 8.7% of the B600. The increased N content was also observed by other researchers [19,27,28]. However, the O content, and the molar ratios of O/C and (O+N)/C decreased significantly with increasing pyrolytic temperature. In particular, the O content declined from 13.2% of raw bagasse to 6.1% of the B600. Accordingly, the decrease in molar O/C ratio indicated that the biochar surface became less hydrophilic with increasing pyrolytic temperature, while the decrease of the polarity index (molar ratio of (O+N)/C) implies the reduction in the number of surface polar functional groups [20,29,30]. The biochar surface became more hydrophobic due to the increased C content and the concurrent decrease in O content with an increase in pyrolytic temperature.

The actual production rates of biochar samples during pyrolysis at different temperatures were investigated (Fig. 2(b)). The production rate of biochar samples decreased from 81.0% at 200 °C, to 20.8% at 600 °C. Typically, a mass loss above 250 °C was attributed to the decomposition of bagasse and the release of vapor containing complex organics mixed with gases (water vapor, CO_2, CO, H_2, CH_4, and heavier hydrocarbons) [31]. This can explain the significant loss of organics and the remaining carbon during pyrolysis.

1-2. FTIR Spectra of Biochars Prepared from Bagasse

The FTIR spectra of raw bagasse and biochar samples prepared

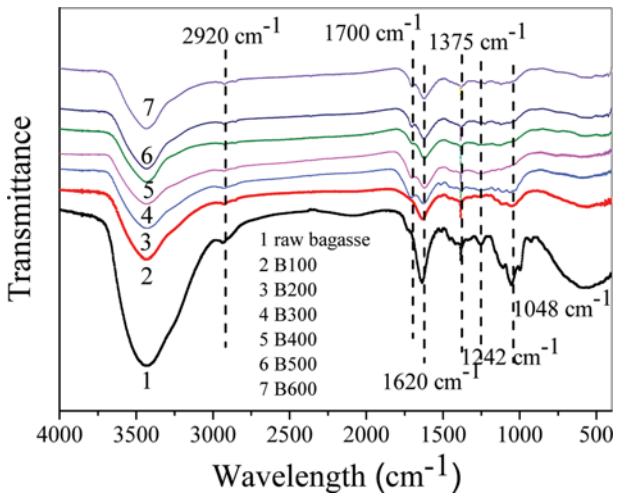

Fig. 3. FTIR spectra of raw bagasse and biochar samples prepared under different pyrolysis temperatures.

at different pyrolytic temperatures are shown in Fig. 3. First, the strong band at 3,439 cm^{-1} represents the stretching vibration of

hydroxyl groups, which became weaker with increasing pyrolytic temperature. This indicated the significant loss of moisture and water of hydration, as a consequence of pyrolysis. Secondly, the bands at 2,920 cm^{-1} (aliphatic C-H stretching) and at 1,048 cm^{-1} (C-O-C) almost disappeared after heating to 400 °C, while the intensities at 1,620 cm^{-1} (aromatic C=C and C=O), 1,375 cm^{-1} (CH_2), and 1,242 cm^{-1} (C-O in the acetyl group) weakened simultaneously [20,32,33]. The aforementioned behavior matched the EDX observations. Finally, the band at 1,700 cm^{-1} (C=O) became better defined, which differed from data found by other studies, as the elimination of the band at 1,700 cm^{-1} was observed by other researchers [32,34]. This implied that the content of C=O functional groups among oxygen-containing functional groups increased while the concentration of other oxygen-containing functional groups diminished concurrently.

2. Effect of Pyrolytic Temperature on Pollutants Uptake

As the functional groups and polarity of bagasse could be altered as a consequence of pyrolysis at different temperatures, the adsorption performance of the resulting biochars was expected to vary. Fig. 4 shows the effect of pyrolytic temperature on the adsorption of p-benzoquinone, tetracycline, and PVA. The uptake of p-benzoquinone, tetracycline, and PVA by B100 reached 3.3, 8.8, and 14.2 mg/g, respectively. By contrast, the uptake of p-benzoquinone, tetracycline, and PVA by B600 reached 18.9, 17.0, and 36.9 mg/g, respectively. Evidently, the affinity of biochars towards p-benzoquinone, tetracycline, and PVA improved with increasing pyrolytic temperature.

On the other hand, besides the surface chemistry disparity of these bagasse biochars, the properties of p-benzoquinone, tetracycline, and PVA vary significantly. It is well accepted that tetracycline is highly water-soluble, while p-benzoquinone is weakly water-soluble and is regarded as an electron acceptor with low polarity. Considering PVA, although it is a water-soluble synthetic polymer, complete dissolution could be achieved by the formation of hydrogen bonds only by heating the solution to over 75 °C. From this point of view, the polarity of the three pollutants in the increasing order is: tetracycline, p-benzoquinone, then PVA. As mentioned, the increased pyrolytic temperature decreased the polarity of these biochars, which actually enhanced the uptake of pollutants with a comparatively lower polarity among the three pollutants by hydrophobic interaction. Accordingly, the increased adsorption of PVA molecules outperformed that of tetracycline and p-benzoquinone from B100 to B600. Concurrently, as a non-ionic hydrophobic organic molecule, the adsorption of p-benzoquinone onto the graphitic surface of the biochar could be inhibited by the surface O-containing functional groups, as the clustered water molecules around the O-groups compete with p-benzoquinone for adsorption sites [35,36]. As a result, a decrease in the number of O-containing functional groups actually improved p-benzoquinone uptake.

3. Effect of Solution pH on Pollutant Uptake

The effect of solution pH on the adsorption of p-benzoquinone, tetracycline, and PVA was investigated (Fig. 5(a)). As stated above, the polarity index (molar ratio of (O+N)/C) decreased from 28.1% of raw bagasse to 19.7% of biochar pyrolyzed at 600 °C, indicating a 29.9% decrease in bagasse polarity. Acidic and neutral pH conditions were favorable to the uptake of p-benzoquinone and PVA, while alkaline conditions (from pH 9.0 to 11.0) led to a decrease in adsorption capacity for both pollutants. However, the adsorp-

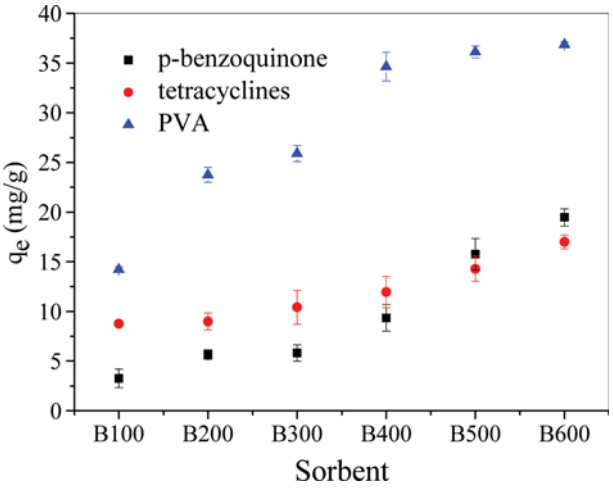

Fig. 4. Effect of pyrolytic temperature on p-benzoquinone, tetracycline and polyvinyl alcohol (PVA) adsorption.

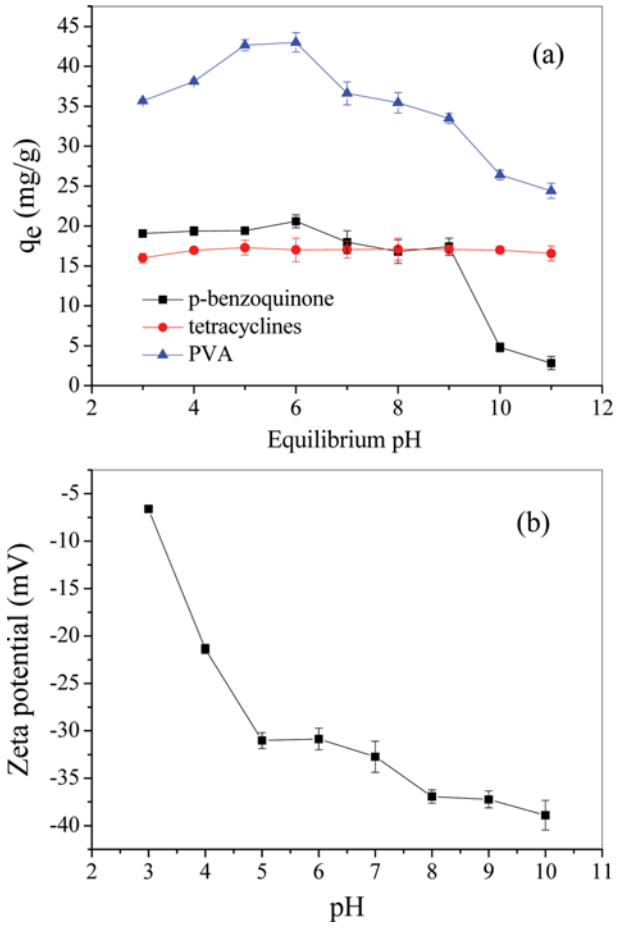

Fig. 5. Effect of solution pH on the adsorption of p-benzoquinone, tetracycline and PVA onto B600 (a) and Zeta potentials of bagasse biochar B600 (b).

tion of tetracycline was unaffected by changes in solution pH. As is known, tetracycline (H_2L) is an amphoteric compound with pK_a values of 3.3, 7.7, and 9.7 [37]. Its predominant species are expected to be cations (H_2L^+) at pH<3.3, zwitterions (H_2L^0) at 3.3<pH<7.7, or negatively charged anions (HL^-, L^{2-}) at pH>7.7. The tetracycline molecules actually became more negatively-charged with increasing solution pH. In this case, it indicated that the effect of electrostatic force seemed not to be dominant.

For the bagasse biochars, they had more graphitized surfaces, and consequently the surfaces were expected to have higher π-electron density. As tetracycline and p-benzoquinone are regarded as π-electron acceptors, and biochar B600 as a π-electron donor, the mechanism of π-π electron-donor-acceptor (EDA) interaction might contribute to the enhanced adsorption of tetracycline and p-benzoquinone onto B600 [38-40]. Meanwhile, as the protonated and neutral species of tetracycline are more effective π-electron acceptors, a slight decrease in tetracycline uptake was expected under alkaline conditions, as proved by the experimental results (Fig. 5(a)). Accordingly, a dramatic decline in p-benzoquinone adsorption might be attributed to the comparatively weaker interactions between p-benzoquinone and the graphitic surface of biochar B600 under alkaline conditions than under acidic and neutral conditions. Finally, H-bond interaction between PVA molecules with abundant OH groups and the surface oxygen groups of B600 is expected to be prevalent during adsorption [40,41]. It can be deduced that PVA molecules became more negatively-charged as the solution pH increased. The zeta potentials of the adsorbent surfaces at different solution pH values are shown in Fig. 5(b). Apparently, the surface of biochar B600 became more negatively-charged, especially at pH>5.0; accordingly, an apparent decrease in PVA uptake was observed at pH>5.0 as a consequence of weaker H-bond interactions between PVA molecules and B600.

4. Adsorption Kinetics and Isotherms

The kinetics and isotherms for the adsorption of p-benzoquinone, tetracycline, and PVA on B600 at 25 °C and neutral solution pH were investigated (Fig. 6). Judging from the kinetic curves (Fig. 6(a)), the adsorption processes exhibited typical three-stage kinetic behavior, with over 50% removal for p-benzoquinone, tetracycline, and PVA occurring in the initial rapid stage (60 min). At the same time, the experimental kinetic data were simulated by non-linear models, including pseudo-first-order, pseudo-second-order, and Elovich models as presented below.

The pseudo-first-order model can be expressed as [42]:

$$q_t = q_e(1-e^{-k_1 t}) \quad (2)$$

The pseudo-second-order model can be expressed as [43]:

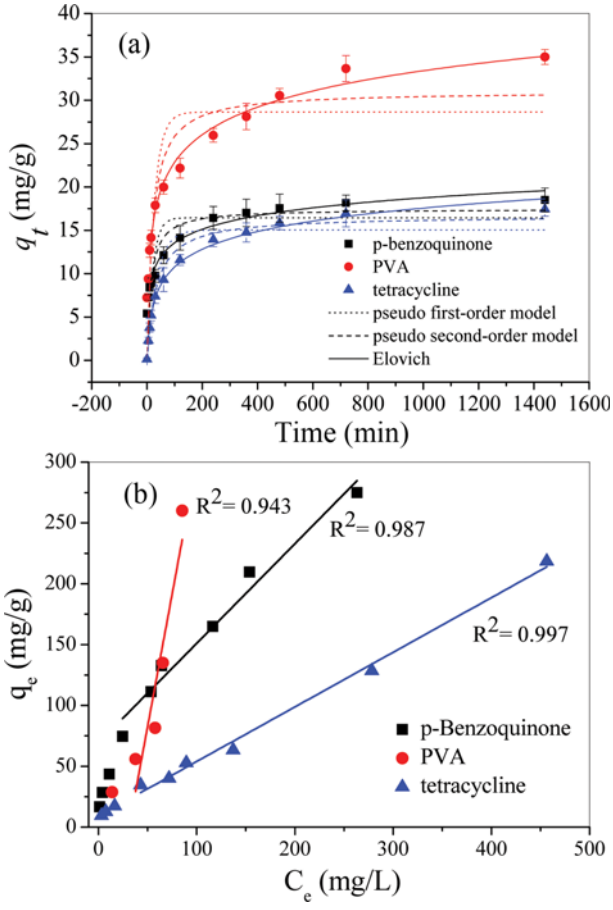

Fig. 6. Kinetics and isotherms for the adsorption of p-benzoquinone, tetracycline and PVA on B600 at 25 °C and neutral solution pH.

$$q_t = \frac{k_2 q_e^2 t}{(1+k_2 q_e t)} \quad (3)$$

The Elovich model can be expressed as [44]:

$$q_t = a + k\ln t \quad (4)$$

where q_e and q_t are the adsorption capacities (mg/g) of the adsorbent at equilibrium and at time t (min), respectively; and k_1 (min^{-1}) and k_2 (g/(mg min)) are the related adsorption rate constants for the pseudo-first-order and pseudo-second-order models, respectively; a and k are the constants in the Elovich equation.

The non-linear kinetic model parameters for the adsorption of p-benzoquinone, tetracycline, and PVA are also listed in Table 1.

Table 1. The non-linear kinetic models parameters for the adsorption of p-benzoquinone (Bq), tetracycline (TC) and PVA on B600 at 25 °C and neutral solution pH

	Pseudo-first-order model			Pseudo-second-order model			Elovich model		
	k_1 (min^{-1})	q_e (mg/g)	R^2	k_2 (g/mg·min)	q_e (mg/g)	R^2	a	k	R^2
Bq	0.048	16.4	0.637	0.0040	17.46	0.770	3.113	2.268	0.852
TC	0.017	15.59	0.948	0.0013	17.19	0.987	2.489	2.897	0.994
PVA	0.038	28.71	0.730	0.0015	31.14	0.841	1.717	4.584	0.932

The values of $q_{e,exp}$ for p-benzoquinone, tetracycline, and PVA were 18.52, 17.40, and 35.02 mg/g, respectively. They are typically higher than those derived from the simulated results. From both the simulated curves and the correlation coefficients (R^2) of the three models, the experimental data were well fitted by an Elovich model for the three pollutants, indicating that the diffusional rate-determining step was more pronounced [45]. This also implied the involvement of multi-layer adsorption and the occurrence of heterospherical diffusion reactions. Fig. 6(b) shows the adsorption isotherms for the three pollutants: these were seen to be largely different. At high concentrations of the adsorbates, the adsorption isotherms for the three organic pollutants were quasi-linear, indicating that partition was the dominant mechanism for B600. By linear simulation, the isotherms for tetracycline and p-benzoquinone were closer to being linear than that of PVA. Meanwhile, as the relative contribution of adsorption increased with increasing pyrolytic temperature, the contribution from the adsorption was shown to be higher than that of partitioning to total sorption for the biochars of orange peel treated under comparatively higher temperatures (>500 °C) [20]. As such, it could be deduced that the contribution of partitioning was also dominant, besides the key contribution of surface adsorption for B600.

CONCLUSION

The increased pyrolytic temperature, under oxygen-limited conditions, from 100 to 600 °C, reduced the sugarcane bagasse biochar to smaller, thinner flakes, while this also significantly slowed the rate of production and made the biochar surface more hydrophobic. The adsorption affinity of biochars towards p-benzoquinone, tetracycline, and polyvinyl alcohol improved with increasing pyrolytic temperature. A mechanism of π-π electron-donor-acceptor interaction might contribute to the adsorption of tetracycline and p-benzoquinone, while an H-bond interaction between PVA and the biochar might be dominant during adsorption. The Elovich kinetic model indicated a pronounced diffusional rate-determining step. During the uptake of these three pollutants, the contribution of partitioning was also dominant alongside that of adsorption.

ACKNOWLEDGEMENT

The authors thank the National Science Foundation of China for their financial support (Grant no. 51378205), and the Foundation for Innovative Experimental Programmes of NCWU (Grant no. HSCX2014054).

REFERENCES

1. X. Yang, R. C. Flowers, H. S. Weinberg and P. C. Singer, *Water Res.*, **45**, 5218 (2011).
2. B. Xing, N. Senesi and P. M. Huang, *IUPAC Sponsored Book Series.*, **2**, 439 (2011).
3. M. A. Shannon, P. W. Bohn and M. Elimelech, *Nature*, **452**, 301 (2008).
4. T. Polubesova, D. Zadaka, L. Groisman and S. Nir, *Water Res.*, **40**, 2369 (2006).
5. R. Andreozzi, V. Caprio, A. I. Nsola and R. Marotta, *Catal Today*, **53**, 51 (1999).
6. L. B. Stadler, A. S. Ernstoff, D. S. Aga and G. L. Nancy, *Environ. Sci. Technol.*, **46**, 10485 (2012).
7. A. Santos, P. Yustos, A. Quintanill, F. García-Ocho, J. A. Casas and J. J. Rodríguez, *Environ. Sci. Technol.*, **38**, 133 (2004).
8. A. Imran and V. K. Gupta, *Nature Protocols*, **1**, 2661 (2007).
9. A. Imran, *Sepn. & Purfn. Rev.*, **39**, 95 (2010).
10. A. Imran, *Chemical Reviews.*, **112**, 5073 (2012).
11. A. Imran, A. T. M. Tabrez and A. Khan, *Environ. Manage.*, **113**, 170 (2012).
12. A. Imran, *Sepn. Purfn. Reviews*, **43**, 175 (2014).
13. L. L. Ji, W. Chen, L. Duan and D. Q. Zhu, *Environ. Sci. Technol.*, **43**, 2322 (2009).
14. S. K. Behera, J. H. Kim, X. J. Guo and H. S. Park, *J. Hazard. Mater.*, **153**, 1207 (2008).
15. J. Lehmann, *Nature*, **447**, 143 (2007).
16. J. W. Lee, B. Hawkins, D. M. Day and D. C. Reicosky, *Energy Environ. Sci.*, **3**, 1695 (2010).
17. M. Ahmad, A. U. Rajapaksha, J. E. Lim, M. Zhang, N. Bolan and D. Mohan, *Chemosphere*, **99**, 19 (2014).
18. M. Keiluweit, P. S. Nico, M. G. Johnson and M. Kleber, *Environ. Sci. Technol.*, **44**, 1247 (2010).
19. Y. N. Sun, B. Gao, Y. Yao, J. Fang, M. Zhang and Y. M. Zhou, *Chem. Eng.*, **240**, 574 (2014).
20. B. L. Chen and Z. M. Chen, *Chemosphere*, **76**, 127 (2009).
21. B. Xing and J. J. Pignatello, *Environ. Sci. Technol.*, **31**, 792 (1997).
22. B. Chen, D. Zhou and L. Zhu, *Environ. Sci. Technol.*, **42**, 5137 (2008).
23. F. Z. Li, G. T. Li and X. W. Zhang, *J. Environ. Sci.*, **26**, 708 (2014).
24. P. H. Chang, Z. Li, W. T. Jiang and J. S. Jean. *Colloids Surf., A Physicochem. Eng. Asp.*, **339**, 94 (2009).
25. J. H. Finley, *Anal. Chem.*, **33**, 1925 (1961).
26. Y. Yao, B. Gao, J. Fang, M. Zhang, H. Chen and Y. M. Zhou, *Chem. Eng.*, **242**, 136 (2014).
27. B. L. Chen and Z. M. Chen, *Chemosphere*, **76**,127 (2009).
28. M. I. Al-Wabel, A. Al-Omran, A. H. El-Naggar, M. Nadeem and A. R. A. Usman, *Bioresour. Technol.*, **131**, 374 (2013).
29. Y. Chun, G. Y. Sheng, C. T. Chiou and B. S. Xing, *Environ. Sci. Technol.*, **38**, 4649 (2004).
30. G. Cornelissen and O. Gustafsson, *Environ. Sci. Technol.*, **39**, 764 (2005).
31. M. J. G. Antal, *Ind. Eng. Chem. Res.*, **42**, 1619 (2003).
32. X. D. Zhu, Y. C. Liu, C. Zhou, G. Luo, S. C. Zhang and J. M. Chen, *Carbon*, **77**, 627 (2014).
33. Z. M. Xi and B. L. Chen, *Environ. Sci.*, **26**, 737 (2014).
34. W. S. Carvalho, D. F. Martins, F. R. Gomes, I. R. Leite, L. G. Silva and R. Ruggiero, *Biomass Bioenergy*, **35**, 3913 (2011).
35. M. Franz, H. A. Arafat and N. G. Pinto, *Carbon*, **38**, 1807 (2000).
36. D. Zhu and J. J. Pignatello, *Environ. Sci. Technol.*, **39**, 2033 (2005).
37. H. J. Liu, Y. Yang, J. Kang, M. H. Fan and J. H. Qu, *J. Environ. Sci.*, **24**, 242 (2012).
38. M. Teixidó, J. J. Pignatello, J. L. Beltrán, M. Granados and J. Peccia, *Environ. Sci. Technol.*, **45**, 10020 (2011).
39. H. Zheng, Z. Y. Wang, J. Zhao, H. Stephen and B. S. Xing, *Environ. Pollut.*, **181**, 60 (2013).
40. X. R. Jing, Y. Y. Wang, W. J. Liu, Y. K. Wang and H. Jiang, *Chem.*

Eng., **248**, 168 (2014).
41. J. Z. Ni, J. J. Pignatello and B. S. Xing, *Environ. Sci. Technol.*, **45**, 9240 (2011).
42. S. Lagergren, *Handlingar*, **24**, 1 (1898).
43. Y. S. Ho and G. McKay, *Process Biochem.*, 3**4**, 451 (1999).
44. D. L. Sparks, Kinetics of Soil Chemical Process, Academic Press, New York (1989).
45. C. Aharoni, D. L. Sparks, S. Levinson and I. Revina, *Soil. Sci. Soc. Am.*, **55**, 1307 (1991).